Optically detected magnetic resonance of epitaxial nitrogen-doped ZnO

G. N. Aliev, S. J. Bingham, D. Wolverson,* and J. J. Davies
Department of Physics, University of Bath, Bath BA2 7AY, United Kingdom

H. Makino, H. J. Ko, and T. Yao
Institute for Materials Research, Tohoku University, 2-1-1 Katahira, Aoba-ku, Sendai 980, Japan
(Received 16 April 2004; published 16 September 2004)

Optically detected magnetic resonance (ODMR) experiments on epitaxial nitrogen-doped ZnO show spectra due to (i) a shallow donor with the full wurtzite symmetry, (ii) a previously unobserved spin-1/2 center of axial symmetry whose principal axis is tilted slightly away from the crystal *c* axis, and (iii) a spin–1 triplet state of orthorhombic symmetry. The spin-1/2 center has a *g* tensor that is of a different form from that of previously reported ODMR spectra for ZnO and is consistent with a model that contains a zinc interstitial, possibly in association with a nitrogen atom. The *g* values for the triplet state are the average of those for a shallow donor and the spin-1/2 center, and the spectrum is thus assigned to a pair of such centers strongly coupled by a spin-exchange interaction.

DOI: 10.1103/PhysRevB.70.115206 PACS number(s): 76.70.Hb, 78.55.−m

I. INTRODUCTION

The wide band-gap semiconductors GaN and ZnO are similar in many fundamental respects, including their crystal structures, lattice parameters, and band gaps. For this reason, the technological successes of epitaxially grown heterostructures based on GaN[1] have stimulated interest also in epitaxial ZnO[2,3] (ZnO has been studied extensively in the form of bulk crystals over several years). The differences between the two materials also provide grounds for interest in ZnO as well as GaN; in particular, the exciton binding energy of ZnO (60 meV) is much larger than that of GaN (21 meV).

Controlled doping of ZnO to produce *p*-type material is essential for many device structures and also for the appearance of ferromagnetism that has been proposed to be achievable in (Zn,Mn)O compound semiconductors.[4,5] Nitrogen has been one of the most successful *p*-type dopants in several II-VI semiconductor systems (for instance, in ZnSe, via liquid phase epitaxy,[6] organometallic chemical vapor deposition,[7] or molecular beam epitaxy[8–10] and in ZnTe[11]). The doping of ZnO via substitutional nitrogen incorporation has therefore become a key topic in current work on ZnO since it was originally proposed.[12] Some other potential acceptors, for instance, arsenic, are also promising[13,14] and some, e.g., lithium, have been studied over many years in both bulk and powder samples.[15–17] Much work remains to be done; for instance, the optimum doping and annealing conditions and particularly the dominant self-compensation mechanism have yet to be established.[18] Recent advances in the epitaxial growth of ZnO and in the use of homoepitaxy and of epitaxy on GaN substrates provide a context for studies of *p*-type doping. Additionally, codoping schemes that may increase the nitrogen activation in ZnO have been proposed and attempted, with controversial results.[19–21]

In the present paper we describe the results of optically detected magnetic resonance (ODMR) experiments on nitrogen-doped ZnO layers produced by plasma-assisted molecular beam epitaxy (MBE). We observe signals from four defect centers in ZnO. We propose a tentative interpretation of the signals in terms of a zinc interstitial, possibly in association with a nitrogen atom, and a strongly exchange-coupled center formed when the zinc interstitial is in close proximity to a shallow donor.

II. EXPERIMENTAL DETAILS

A. Details of the specimens

The samples were grown by plasma-assisted molecular beam epitaxy on *c*-plane sapphire substrates; further details of the growth and characterization of the layers are given in Ref. 2. The nitrogen concentration in the sample used in the present work was estimated to be 10^{19} cm^{-3} though the resistivity was too high to measure the active nitrogen concentration directly by Hall experiments. Some ODMR measurements have been carried out on samples of lower nitrogen concentration and on undoped samples.

B. ODMR technique

ODMR has been widely applied to the investigation of recombination processes in semiconductors. The key feature is that the recombination often involves spin selection rules, so that the intensity or polarization characteristics of the accompanying photoluminescence (PL) depend on the spin distribution within the states that participate in the recombination processes. In the simplest case, increases in the intensity of the PL are observed when magnetic resonance occurs in the excited state, but, in many materials, the behavior is often observed to be more complicated, with luminescence-quenching magnetic resonance signals being observed when, for example, resonance causes the transfer of carriers into a process competing with the PL band that is being monitored. The signals of interest in the present work are of the luminescence-enhancing type. For recent reviews of ODMR in wide band-gap materials, see Refs. 22 and 23.

The present investigation was carried out with microwave frequencies in the 14 and 33 GHz bands and powers of ~50 and ~60 mW, respectively, and with the specimen in direct contact with superfluid helium in a superconducting magnet. The microwave resonators (in the absence of a sample, $Q \sim 3\,000$) were of rectangular TE_{011} form with appropriate optical access and could be rotated about an axis perpendicular to the magnetic field. The PL was excited with the multiline UV output of an argon-ion laser (363.8 and 351.1 nm, 3.41 and 3.53 eV), giving photon energies close to the band gap of ZnO (3.44 eV at 1.6 K). Typical excitation powers were in the region of 10 mW. The entire sample surface (of area about 10 mm^2) was illuminated without focusing, giving a typical illumination intensity of 0.2 W cm^{-2}. The incident microwaves were chopped at frequencies in the range 200 Hz to 10 kHz and changes in the PL intensity were monitored with an S20 response photomultiplier and a lock-in amplifier; the modulation of the PL under magnetic resonance conditions was in the range 0.1–0.01%. The PL emitted either along or at right angles to the magnetic field was monitored and, for ODMR, suitable parts of the spectrum were selected through use of combinations of high- and low-pass interference filters; a filter blocking wavelengths shorter than 400 nm was permanently in place in order to reject the excitation light.

C. Photoluminescence measurements

PL spectra were recorded in a separate system using HeCd laser excitation (325 nm) with the sample held at 10 K in a closed-cycle cryostat. Where necessary, a type Wratten 18A absorbing filter or a 325 nm dielectric mirror was used to remove plasma lines in the visible region from the excitation laser beam. For the visible spectral region, a type GG400 absorbing filter was also used in front of the spectrometer to eliminate light of wavelength shorter than 400 nm, which was otherwise transmitted in second order.

III. EXPERIMENTAL RESULTS

A. Photoluminescence spectra

The photoluminescence spectrum of the ZnO:N sample used in this work is typical of epitaxial material grown under the conditions described in Ref. 2 and is shown in Fig. 1. The dominant, sharp line at 3.357 eV is due to bound exciton recombination (the line shows partly resolved structure and its exact origin is not clear) and, on its low-energy side, is accompanied by weak signals ascribed to phonon replicas (with characteristic separation of about 71 meV).[24] Weak shallow donor-shallow acceptor pair recombination emission is also observed between 3.1 and 3.3 eV. At lower energies still, a band is observed covering most of the visible spectral region. This band extends over the wavelength range of the PL band associated with copper centers in ZnO (Ref. 25) but, as has been discussed in the case of undoped epitaxial ZnO, we do not assign this band to the presence of copper, since the characteristic phonon structure of the Cu^{2+} center is not observed.[26–29] In principle, unstructured PL spectra in the green region may be related to donor-acceptor pair recombination involving Cu^{+} acceptors.[30] However, we believe that there is no serious copper contamination in our material since no secondary ion mass spectrometry (SIMS) signal from this element was detected in undoped ZnO layers (the detection limit was around 10^{15} cm^{-3}) and since the growth environment was kept the same for the N-doped ZnO layers. Furthermore, our ODMR spectra described below show no evidence of copper-related signals.

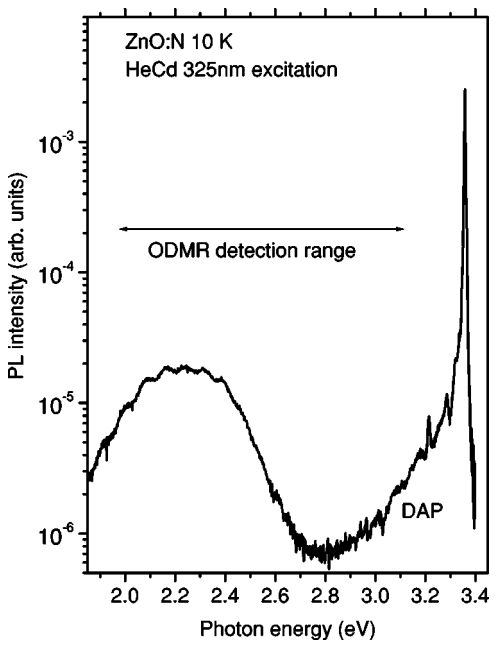

FIG. 1. 10 K photoluminescence spectrum of the ZnO:N sample using 325 nm (HeCd) excitation. The spectrum is not corrected for the system spectral response. The detection range of the ODMR experiments is indicated by the horizontal arrow.

B. Overview of the ODMR spectra

Typical ODMR spectra are shown in Fig. 2 for two laser excitation powers (differing by a factor of 100) at 13.76 GHz and with the magnetic field oriented along the crystal *c* axis. Five lines are seen in spectrum (a), which was recorded with the highest laser power. The dependence of these signals on laser power is quite different so that, for example, the signals (*T*) at magnetic fields of 0.4927 and 0.4954 T have similar power dependences and thus appear likely to be related to one another but can be distinguished from signal *U* at 0.4895 T. We therefore infer the existence of four centers (*Z*, *U*, *T*, and *D*) that contribute to this spectrum, as labeled in Fig. 2. We do not find a marked dependence of the spectra on the microwave modulation frequency, the microwave power, or the detection wavelength range employed (indicated on Fig. 1) and so are unable to distinguish between the different signals on this basis.

1. Shallow donor signal (center D)

The signal observed at 0.5022 T in Fig. 2 (center *D*) is found to be anisotropic, with a magnetic-field-induced splitting ΔE of the spin states described by the expression[31]

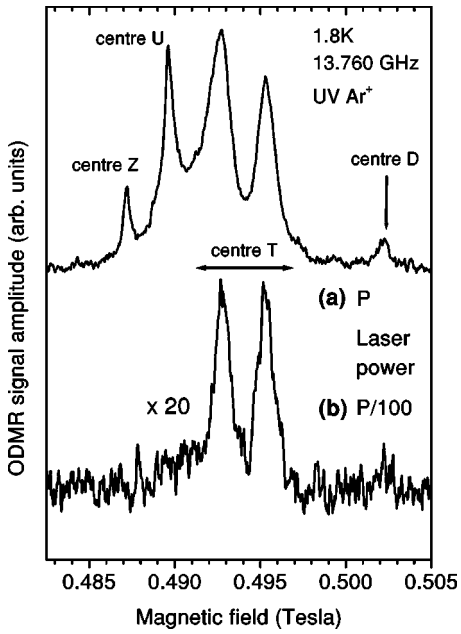

FIG. 2. ODMR spectra of ZnO:N for 13.76 GHz microwave excitation with optical powers of (a) 10 mW and (b) 0.1 mW at 1.8 K and with UV Ar^+ optical excitation, detected using the whole visible spectral region (wavelengths in the range 400–700 nm). Spectrum (b) has been multiplied by a factor of 20, and the spectra are displaced vertically for clarity. The positive vertical direction corresponds to an enhancement of the PL signal.

$$\Delta E = \mu_B B \sqrt{g_\perp^2 \sin^2(\theta) + g_\parallel^2 \cos^2(\theta)}. \quad (1)$$

Here, θ is the angle between the magnetic field **B** and the *c* axis and μ_B is the Bohr magneton. The values of $g_\perp$ and $g_\parallel$ are given in Table I and correspond to those previously reported from electron spin resonance (ESR) and ODMR studies of shallow donor centers in ZnO. Shallow donors are known to be formed by incorporation of gallium[32,33] or indium,[33,37] though in each case the magnetic resonance signal is broadened or even split because of hyperfine interactions. In the former case, the gallium hyperfine interactions result in a line broadening of about 2 mT,[32,33] whereas, for indium, the coupling between the ^{115}In nucleus (spin $I=9/2$) leads to ten components spanning a range of 30 mT.[33,37] In the present experiments, the linewidth is about 1 mT, which excludes indium and probably also gallium as the source of the donor impurity. Other possible sources would, as in other II-VI materials, be aluminum or halogen impurities (for which the hyperfine interactions would be small). Hydrogen is also now well established in both theoretical[34] and experimental[35,36] studies to be a shallow donor in ZnO, with an activation energy of 35 meV and with *g* factors close to those given in Table I for shallow donors.[36] We do not have information on the hydrogen content of the present samples. However, while we cannot identify the nature of the impurity (or defect) that gives rise to the donor signal, we note that, since it is observed in undoped ZnO layers grown by the same technique, there is no reason to suppose that it is related to the nitrogen doping.

2. Spin=1/2 signal (center U)

The signal seen at a magnetic field of 0.4895 T in Fig. 2 (center *U*) is slightly anisotropic and moves to a higher field when the field direction is away from the *c* axis. To a first approximation the behavior can be described by Eq. (1), though spectra taken at 33 GHz (see Sec. III C below) provide evidence for a small splitting of the signals for field orientations away from the *c* axis. This splitting cannot be investigated fully because of overlap of the spectra with that due to center *Z* when θ approaches $\pi/2$ [see Figs. 4(a) and 4(b)]. In a specimen with lower nitrogen concentration, signals from center *U* were not observed, even though those

TABLE I. Summary of the spin-Hamiltonian parameters required to fit the ODMR spectra of nitrogen-doped zinc oxide, together with some previously reported values. The centers listed are in ZnO unless specified otherwise.

Center (this work)	$g_\perp$ or (g_x,g_y)	$g_\parallel$ or g_z	$\lvert D\rvert$ (μeV)	$\lvert E\rvert$ (μeV)	*z* axis (angle to *c*)	Assignment
D	1.9556	1.9574	...	...	0°	shallow donor (see Sec. III B 1)
	1.96	1.96	...	...	0°	halogen donor (Ref.15)
	1.9556 to 1.9562	1.9574	...	...	0°	Ga, In shallow donors (Refs. 33 and 37)
	1.9551	1.9570	...	...	0°	shallow donors (Ref. 28)
T	(1.983,1.982)	1.9894	0.15	0.12	0°	$S=1$ (see Sec.III C)
	2.0224	1.9710	3.16	...	0°	$S=1$(Ref.28)
	2.025	1.984	3.20	...	0°	O vacancy $S=1$ (Ref. 29)
Z	2.006	2.020	...	...	20°	$S=1/2$ (see III C)
	2.052	2.006	...	...	0°, 109°	ZnS *A* center (Ref. 38)
	(2.0223,2.0254)	2.0040	...	...	0°, 109°	Li acceptor (Ref. 16)
	(2.0173,2.0183)	2.0028	...	...	69.2°	Zn vacancy (Ref. 39)
	1.996	1.995	...	...	0°	O vacancy (F^+ center) (Refs. 40 and 41)
	1.9633	1.9953	...	...	0°	N acceptor (Ref. 28)
U	2.0060	2.0076	...	...	0°	$S=1/2$ (see Sec. III B 2)

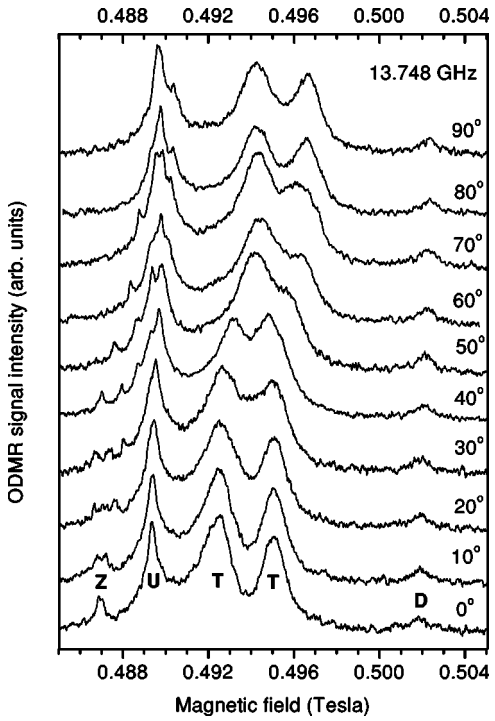

FIG. 3. ODMR spectra of ZnO:N for 13.748 GHz microwave excitation for a series of angles (indicated on the figure) between the magnetic field and the crystal *c* axis, where the magnetic-field vector is in a plane of form $\{10\bar{1}0\}$.

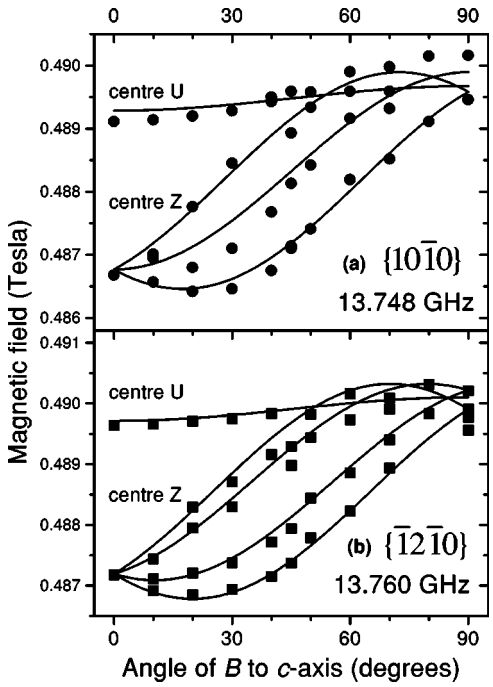

FIG. 4. Dependence of line positions of the ODMR signals arising from centers *Z* and *U* on the direction of the magnetic field in (a) a $\{10\bar{1}0\}$ plane and (b) a $\{\bar{1}2\bar{1}0\}$ plane. Solid lines: calculated angular dependences according to the models discussed in Secs. III B 2 and III C 1. The experimental data (shown by solid circles and squares) were obtained by decomposition of the spectra using Lorentzian line shapes.

from center *Z* were detected: centers *U* and *Z* are therefore distinct.

C. Angle dependence of the ODMR signals from centers *T* and *Z*

The behavior of centers *T* and *Z* as the magnetic field is rotated away from the high symmetry *c* axis is more complicated than that described above for centers *D* and *U*. In particular, it will be seen that it is necessary to specify the rotation angle of the magnetic field within the crystal *a* plane.

Figure 3 shows a series of ODMR spectra for a sample rotated such that the magnetic field moves (in terms of hexagonal Miller-Bravais indices) in a plane of the form $\{10\bar{1}0\}$. It is useful here to consider the symmetry of the C_{6v} (6 *mm*) point group in some detail. It contains two nonequivalent sets of three mirror planes, forms $\{10\bar{1}0\}$ and $\{\bar{1}2\bar{1}0\}$. The planes of the latter set contain two tetrahedral bonds and those of the former only one (along [0001]). There are six general symmetry-related vectors of the type $\langle 10\bar{1}x\rangle$ (for a given *x*) lying in the set of mirror planes of form $\{\bar{1}2\bar{1}0\}$ and, if the magnetic field is rotated in one of these planes, the directions of these six vectors make *four* distinct angles to the magnetic field at any given rotation angle θ. If, however, the magnetic field is rotated in a mirror plane of the other set $\{10\bar{1}0\}$, then *three* distinct angles now exist between the directions of **B** and the same general vectors.

1. Spin=1/2 signal (center Z)

These considerations are the key to understanding the structure of center *Z*. From Fig. 3, it can be seen that the single line observed near $B=0.487$ T for $\theta=0°$ splits into three components and moves to higher magnetic-field values. Although it then overlaps the signals of center *U*, fitting of all the data of Fig. 3 is possible and the results are summarized in Fig. 4(a). Note that, in parts 4(a) and 4(b) of this figure, slightly different microwave frequencies were used so that the zero-angle lines appear at slightly different magnetic fields. The fitted curves are calculated taking this into account and using the same spin-Hamiltonian parameters for 4(a) and 4(b). We have recorded analogous spectra for the case where the magnetic field is rotated in the orthogonal plane and find that four signals are now observed. The results of fitting these spectra are shown in Fig. 4(b).

These observations show that center *Z* has a spin of $S=1/2$, giving rise to a single ODMR transition, but that its principal axis is tilted away from the *c* axis and lies in a plane of form $\{\bar{1}2\bar{1}0\}$. Centers of each of the six symmetry-related orientations give rise to separate contributions to the ODMR spectrum and, therefore, three or four signals are observed depending on the rotation plane. ΔE is again of the form of Eq. (1) but the axis along which $g_{\|}$ is defined must be determined by numerical fitting of the data of Fig. 4 and is found to be oriented at approximately 20° to the *c* axis. This angle can already be estimated by inspection of Fig. 4(b), since it is the angle at which the lowest-lying ODMR transition has its minimum value.

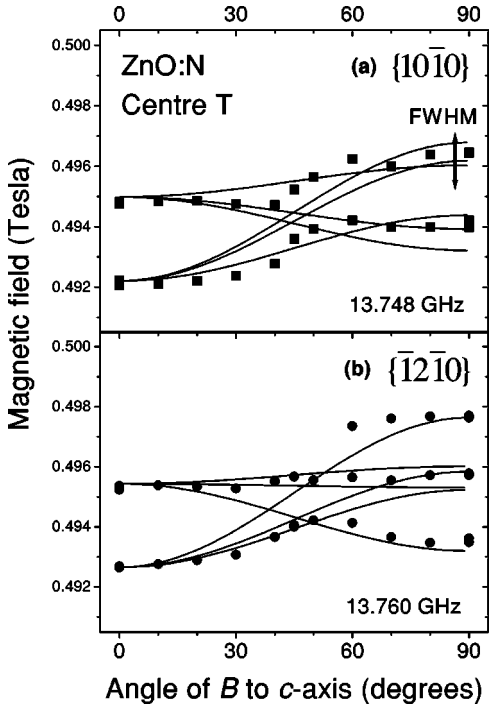

FIG. 5. Dependence of line positions of the ODMR signals arising from center T on the direction of the magnetic field in (a) a $\{10\bar{1}0\}$ plane and (b) a $\{\bar{1}2\bar{1}0\}$ plane. Solid lines: calculated angular dependences according to the models discussed in Sec. III C 2. The experimental data (shown by solid circles and squares) were obtained by decomposition of the spectra using Lorentzian line shapes.

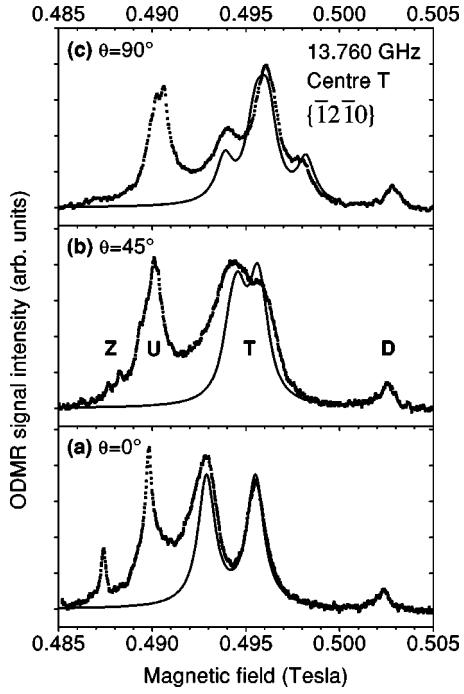

FIG. 6. Dotted lines: ODMR spectra of ZnO:N for 13.76 GHz microwave excitation for angles between the magnetic field and the crystal c axis of (a) 0°, (b) 45°, and (c) 90°. Solid lines: results of simulations of the spectra of center T as discussed in Sec. III C 2.

2. Spin=1 signal (center T)

The remaining lines in the spectra are those belonging to center T. Figure 3 shows that two broad resonances with a full width at half maximum (FWHM) of at least 1 mT are observed at $B=0.4925$ and 0.4950 T for $\theta=0°$ with the magnetic field lying in the plane $\{10\bar{1}0\}$. These resonances approach one another as θ increases and move apart again as θ reaches 90°. This angle dependence is summarized in Fig. 5. For the orthogonal rotation plane $\{\bar{1}2\bar{1}0\}$, Fig. 6(c) shows that three broad resonances are now observed when $\theta=90°$.

The observation of two lines when the magnetic field is parallel to the c axis requires at least a spin of $S=1$ together with a term yielding a small zero-field splitting (in conventional notation, the magnitude of this term is expressed by the parameter D; for a discussion, see Ref. 31). The effective Hamiltonian describing center T is given in Eq. (2). The anisotropy with respect to rotation of the crystal about the c axis, which gives rise to the differences observed between the rotation planes $\{10\bar{1}0\}$ and $\{\bar{1}2\bar{1}0\}$, implies a further reduction in symmetry from tetragonal to othorhombic and this is generated by the final term in Eq. (2), involving the parameter E[31]

$$H = g_x\mu_B S_x B_x + g_y\mu_B S_y B_y + g_z\mu_B S_z B_z + D\left[S_z^2 - \frac{1}{3}S(S+1)\right] + E(S_x^2 - S_y^2), \qquad (2)$$

where the z direction is along the c axis and x is along the crystallographic $[10\bar{1}0]$ direction. The solid lines in Fig. 5 show the magnetic fields at which ODMR resonances are predicted on the basis of Eq. (2). Clearly, more transitions are predicted than are resolved. However, the experimental linewidth is significant; the full width at half maximum of the signals from center T is evident from Fig. 3 and is indicated by the vertical arrow on Fig. 5. If even the simplest possible simulation of the experimental data is carried out, in which all transitions are assumed to have (i) constant and equal intensities and (ii) a Lorentzian line shape of linewidth 1 mT, then the experimental spectra of Fig. 3 are reproduced well at all angles.

Figure 6 shows three such simulated spectra, for angles of $\theta=0°$, 45°, and 90°. Note that the relative intensities of the three lines shown in Fig. 6(c) are well reproduced by this simulation. For example, the high intensity of the central line in Fig. 6(c) arises because of the overlap of four separate contributions at $\theta=90°$, as shown in Fig. 5(b). Despite its simplicity, this model is therefore capable of predicting the spectra of center T at all orientations of the magnetic field with respect to the crystal axes.

D. ODMR results at 33 GHz

In order to test the assignment of the overlapping signals of centers Z and U, and to test the simulation of the spectra of center T, we have obtained ODMR spectra at the higher microwave frequency of 33 GHz. Representative spectra are shown in Fig. 7 (we show here spectra as a function of θ only for the case that **B** lies in the plane $\{\bar{1}2\bar{1}0\}$ though we have obtained data also for the orthogonal orientation).

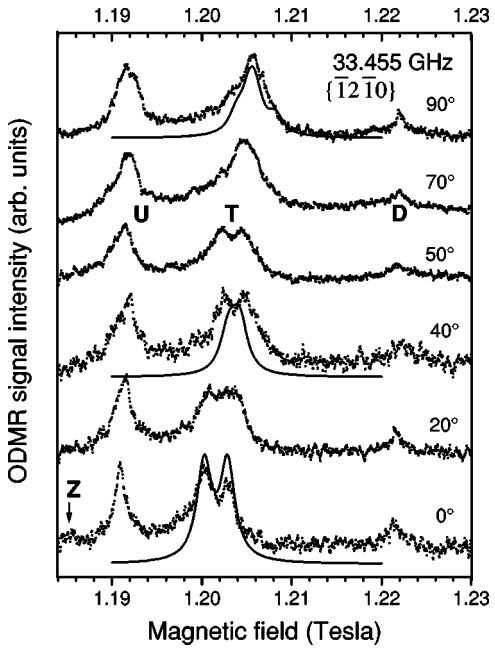

FIG. 7. Dotted lines: ODMR spectra of ZnO:N for 33.455 GHz microwave excitation for a series of angles (indicated on the figure) between the magnetic field and the crystal *c* axis. Solid lines: results of simulations of the spectra of center *T* as discussed in Sec. III C 2.

First, we note that both centers *D* and *U* behave as expected of spin $S=1/2$ centers described by Eq. (1); they appear at magnetic fields which have increased in proportion to the microwave frequency, though it appears that the signal due to center *U* broadens slightly and becomes asymmetric, suggesting unresolved splitting. The poorer signal-to-noise ratio of the 33 GHz spectra, relative to those at 14 GHz, makes the identification of signals from center *Z* more difficult, but the signal for $\theta=0°$ is clear and is found at the magnetic field predicted by the model of Sec. III C 1.

In contrast, the signals assigned to center *T* do not scale with the microwave frequency in a simple way. This is particularly obvious for $\theta=90°$ (Fig. 7), where a single very broad line with a shoulder to lower magnetic field is observed. This spectrum is very different from the corresponding spectrum of Fig. 3, where two well-resolved peaks are seen. The same simulation procedure (with the same parameters as at 14 GHz) has been carried out, and though the agreement with experiment is not so good at $\theta=40°$, the simulation reproduces the principal observation that the main peaks in the spectrum have *converged* as the microwave frequency is increased. This is exactly as expected for a triplet state, since the zero-field splitting becomes progressively negligible as the magnetic field needed to achieve resonance is increased. The results at 33 GHz thus provide significant additional support for the model of Eq. (2). The parameters of all the spin Hamiltonians discussed above are summarized in Table I, together with selected values from the literature.

IV. DISCUSSION

A. Interpretation of the $S=1/2$ spectra, center *Z*

The observation of a spin $S=1/2$ center with *g* values greater than 2 suggests a hole state whose wave function is not predominantly composed of band-edge states; it is well established that the orbital angular momentum of a hole in a single *p*-like state is quenched and results in a spin of $S=1/2$, with *g* factors greater than but close to the free-electron value.[42] One example is the deep acceptor formed in lithium-doped ZnO, where a hole may be trapped in an oxygen *p* orbit oriented along any of the four Li-O tetrahedral directions; since the bond along the *c* axis is not equivalent to the other three, two types of center result.[16,17] A second example is the zinc vacancy in ZnO (Ref. 39) where, again, axial and nonaxial versions of the center are observed.

A more complex defect also giving this type of ODMR signal is the *A* center,[43] in which a zinc vacancy is associated with a donor that may be either a halogen impurity on a group VI site or a group-III metal on a zinc site.[45] A good example of an *A* center is observed in hexagonal ZnS:[38] a Cl impurity is paired with a zinc vacancy and a hole is trapped in a *p* state on a sulfur atom adjacent to the vacancy. The parameters for this center are included in Table I. Similar centers are also observed in ZnSe.[44]

A centers are known to act as deep acceptorlike centers in II-VI compounds such as ZnS and ZnSe, so that recombination of electrons with the holes at the *A* centers leads to broad emission bands well below the band-gap energy. The recombination is subject to spin selection rules, which makes it possible to observe strong ODMR signals.[38] In an *A* center, the presence of the impurity removes the degeneracy of the *p* orbits of the group VI ion adjacent to the zinc vacancy and the hole occupies the lowest-lying orbit, denoted p_z (where *z* is the direction from the chalcogen to the impurity). The shift of the *g* value from the spin-only value is caused by spin-orbit-induced mixing of the p_z state with the higher-lying p_x and p_y. The behavior has been discussed in Refs. 45 and 16. Neglecting any small difference between g_x and g_y, the shifts Δg_i of g_i from g_0 are given by the following approximations, in which λ_p is the spin-orbit coupling constant for the chalcogen species (λ_p is negative for a hole) and ΔE_b is the (positive) splitting in energy between the lowest-energy p_z orbital and those orthogonal to it. Defining *z* as the axial direction of the center (along which $g_\parallel$ is measured),

$$\Delta g_z = \Delta g_\parallel = -2\frac{\lambda_p^2}{\Delta E_b^2}, \tag{3}$$

$$\Delta g_{x,y} = \Delta g_\perp = \frac{-2\lambda_p}{\Delta E_b} - \frac{g_0\lambda_p^2}{\Delta E_b^2}. \tag{4}$$

These formulas are discussed in detail by Schneider *et al.*[45] in the context of ZnS and ZnSe, and are found to give satisfactory explanations of the *g* values. In the case of ZnO, there appear to be no reports of *A* centers of the type observed in ZnS and ZnSe. However, in ZnO, the Li-related center discussed above acts as a deep acceptor[45] and leads to strong ODMR spectra.[17] For a hole trapped in an oxygen *p* orbit, λ_p is estimated to be about −16 meV.[16] With a value for ΔE_b of 1.71 eV, good agreement was obtained between the observed and calculated *g* values,[15] the terms involving λ_p^2 being negligible. Holes trapped at oxygen ions adjacent to zinc vacancies have also been studied by ESR;[39] here again,

$g_x \approx g_y > g_z$. Note that, for *A* centers, for the lithium-containing centers and for the zinc vacancy centers, in each case $g_\parallel \sim 2$ and $g_\perp > g_\parallel$ (see Table I).

The new center (center *Z*) clearly differs from the above examples. First, the relative magnitudes of $g_\perp$ and $g_\parallel$ are reversed. Second, the principal axis of center *Z* lies in a mirror plane containing the *c* axis but is tilted at 20° away from the *c* axis. No evidence is seen for the existence of centers of this type but oriented at 20° to the other three tetrahedral bond directions.

We begin by assuming for the present that center Z does indeed consist of a hole occupying a 2*p* orbit of an oxygen ion. To satify the condition $g_\perp < g_\parallel$, the p_z orbital must now be the highest in energy, so that the hole orbit lies in a plane normal to *z* and is, say, p_x. We then obtain $g_x = 2.0$, $g_y = 2.00 - (2\lambda_p/\Delta_z)$, and $g_z = 2.00 - (2\lambda_p/\Delta_y)$ with $\Delta_{y,z}$ being the energies of $p_{y,z}$ relative to p_x. Substituting the observed values of $g_\perp$ and $g_\parallel$, and taking λ_p to be −16 meV,[16] this model requires that $\Delta_y \simeq 1.6$ eV and $\Delta_z \simeq 5$ eV. These values are implausibly large. It is furthermore difficult to construct a model involving a hole in an oxygen orbital in which the hole is repelled by the neighboring point defect (which would have the required effect of making p_z highest in energy) since there is then no attractive potential to localize the hole. This model thus appears to be incapable of explaining the observed signals.

Similar arguments apply to a hole trapped in a *p* orbital of a nitrogen atom and so this model is also ruled out. A second argument against the assignment of the signal to a center directly involving nitrogen is that no hyperfine splitting of the lines of the present center is observed. In the case of nitrogen in annealed or electron-irradiated bulk ZnO, an ODMR signal has been observed that was attributed to an isolated nitrogen acceptor (the hyperfine interaction with the 99.6% abundant $I=1$ nitrogen nucleus could be resolved and suggested that the wave function of the unpaired spin was of predominantly axial, *p*-like character[28,46]). Electron paramagnetic resonance (EPR) studies of ZnO:N have revealed another nitrogen configuration, the molecular nitrogen acceptor N_2^- and this center is again recognized by its hyperfine structure.[47]

We therefore seek models in which nitrogen plays no *direct* role and in which the hole does not occupy a *p* orbital but occupies instead a *d* orbital. One such possibility is that the center involves an interstitial zinc atom in an approximately octahedral site, Zn_i. The 3*d* states of zinc will be split by the crystal field into a triplet state t_{2_g} and a doublet e_g, of which the doublet is lower in energy by an amount Δ_d; this is analogous to the case of Cu^{2+} in an octahedral field, which is discussed in detail in Sec. 7.16 of Ref. 31. Note that a trigonal distortion of the octahedral site is intrinsic to the wurtzite ZnO structure (since its lattice parameter ratio c/a is not that of ideal hexagonal close packing) but this distortion does not remove the degeneracy of the doublet ground state. However, a further, tetragonal distortion of the center may be expected via the Jahn-Teller effect and does lift this degeneracy; defining Cartesian coordinates *x*, *y*, and *z* along lines joining oxygen ions at opposite apices of the octahedron, expressions similar to those of Eq. (3) may be used to estimate the *g* factors of the center. From Table 7.22 of Ref. 31, these are $g_\perp = 2.00 - (2\lambda_d/\Delta_1)$ and $g_\parallel = 2.00 - (8\lambda_d/\Delta_0)$, where λ_d is the spin-orbit splitting for a hole in a 3*d* orbit (and is negative); Δ_0, Δ_1 are the separations of the new ground state from the states derived from the t_{2_g} state, which is likewise split by the tetragonal distortion. We are able to reproduce the experimentally observed values of $g_\perp$ and $g_\parallel$ given these expressions, and require $\Delta_d \simeq \Delta_0$, Δ_1, and $\lambda_d/\Delta_d \simeq -0.0025$. Using a realistic estimate of −100 meV for λ_d,[48] this would imply a value of Δ_d of about 40 eV. This is much larger than typical figures for the crystal field of an oxygen octahedron (1.5–2.5 eV)[48,49] and so we rule out the possibility of a hole in a pure 3*d* orbit.

Instead, we propose that the center consists of a zinc interstitial Zn_i^+ with substantial hybridization between 3*d* and 4*s* levels. We write the hole wave function as $\Phi = \alpha\phi_{4s} + \beta\phi_{3d}$, where $\alpha^2 + \beta^2 = 1$ and the electronic configurations contributing to the hybridization are represented by $\phi_{4s} = (3d)^{10}(4s)^1$ and $\phi_{3d} = (3d)^9(4s)^2$. The resulting *g* factor is given by $g = \alpha^2 g_{4s} + \beta^2 g_{3d}$, with g_{3d} given by the expressions for $g_\perp$ and $g_\parallel$ in the preceding paragraph and the isotropic term $g_{4s} = 2$. This yields

$$g_z = g_\parallel = 2 - \left(\frac{8\lambda_d}{\Delta_d}\right)\beta^2, \tag{5}$$

$$g_{x,y} = g_\perp = 2 - \left(\frac{2\lambda_d}{\Delta_d}\right)\beta^2. \tag{6}$$

Taking values of −100 meV for λ_d and 2 eV for Δ_d, for example, we can now reproduce the experimental values of $g_\perp$ and $g_\parallel$ if we assume a value of $\beta^2 \simeq 0.05$, so that the hole orbital would have a predominantly 4*s* character with only a small admixture of the 3*d* state, which appears plausible. In this simple picture, the only experimental observation not satisfactorily accounted for is that the *z* direction (in which $g_\parallel$ is obtained) would lie along a line between two apical oxygen atoms of an approximate octahedron and would thus be tilted at around 55° to the crystalline *c* axis, rather than the 20° that we observe. However, the trigonal and tetragonal distortions that we must assume in this model will be expected to alter this angle. Note that, given the present signal strength, we would not necessarily expect to detect the possible hyperfine structure due to the 4.1% abundant isotope ^{67}Zn (nuclear spin $I=5/2$).

In the above discussion, it was assumed that the zinc interstitial is isolated. The simplest model for the recombination process that leads to the ODMR signals is thus $(D^+ + e^-) + Zn_i^+ \rightarrow D^+ + Zn_i^0$, where D^+ represents an unidentified shallow donor. The analysis assumed that the reduction in symmetry is caused by a Jahn-Teller distortion. An argument against this is that the admixture of *d* states is weak, so that the energy reduction gained by a distortion would be small. An alternative possibility is that the reduction in symmetry is instead caused by the presence of an impurity close to the zinc interstitial. A candidate would be nitrogen, lying at an oxygen site. The nitrogen would need to be nonmagnetic, presumably in the trivalent state. Thus, the complex $Zn_i^+ - N_o^-$ would take the place of Zn_i^+ in the recombination process above. Following recombination, the complex would

become $Zn_i^0 - N_o^-$. At first sight, this would appear unlikely, since one might expect complexes in which N_O^0, rather than N_O^-, to be more stable, but the possibility cannot be excluded. There is recent evidence from studies of electron-irradiated ZnO that Zn interstitials do exist and are mobile at room temperature;[50] this implies that isolated Zn_i centers would be unlikely to persist in our samples and does therefore suggest that the signals we observe arise from a complex of which Zn_i is only a component.

The possible presence of zinc interstitials in ZnO was proposed many years ago[51] and remains a subject of discussion; zinc interstitials are often invoked in models for the green PL emission from ZnO (though they are not the only possible candidate[29]). The *n*-type conductivity of bulk ZnO crystals was attributed to Zn_i forming a shallow donor (arguments against the alternative suggestion of oxygen vacancies were given).[51] However, no ESR signals of the Zn_i^+ center could be detected.[52] Vacancy centers, on the other hand, can be demonstrated to exist by other means, for example, positron lifetime studies.[53] The evidence for the existence of zinc interstitials in related systems is clearer; for instance, it is well established in ZnSe.[54–56] It also seems likely that sample treatments such as electron bombardment can generate Zn_i;[50,57] however, this may generate many types of defect simultaneously and, for example, is proposed also to generate F^+ (i.e., oxygen vacancy) centers.[41] Recently, a number of *ab initio* calculations of the formation energies of point defects in ZnO have been carried out. There is general agreement that, under *p*-type doping conditions, the oxygen vacancy has a low formation energy, but the question of whether this or the zinc interstitial are the dominant native shallow donor does not appear to be resolved.[58,59] The possibility that a zinc antisite defect is also present has also been raised.[60] Most recently, a link has been proposed between Zn_i^+ and the green PL emission band owing to the change in PL intensity on the application of an electric field to ZnO single crystals; this change was attributed to the drift of zinc interstitials.[61] In summary, there are several indirect suggestions of the existence of zinc interstitials in ZnO. The signals described in this section and assigned to Zn_i^+ (either isolated or within a complex) clearly require more detailed investigation but may lead to the resolution of this question.

B. Interpretation of the $S=1$ spectra, center T

Deep centers of spin $S=1$ are a relatively common observation in the ODMR of photoluminescence bands at low energies with respect to the semiconductor band gap. For example, it is sometimes the case that a shallow donor and a deep acceptor are in sufficiently close proximity for the exchange interaction to be sufficiently large for the combined spin states to form a spin triplet and a singlet, separated in energy by an amount that is large compared with the Zeeman splittings and the microwave quantum. Under such circumstances, only the transitions between the levels of the triplet state are observed. The g factor in the triplet state tends to $(g_A+g_D)/2$, where g_A and g_D are the g factors of the acceptor and donor, respectively.[62,63] Because the host lattice in the present case is wurtzite and also because the pair of centers has lower symmetry than the lattice itself, there are likely to be additional low-symmetry interactions which lead to the additional zero-field splitting terms (involving D and E) in the spin Hamiltonian of Eq. (2) for the triplet state. We therefore explore the possibility that the type T spectrum is indeed due to recombination between shallow donors and deep acceptors.

Inspection of the values of the parameters for center T (Table I) shows that its g factors are very close to the average of those measured for centers D (the shallow donor) and Z (the proposed zinc interstitial, so that, for a particular direction of the field, $g_D+g_Z=2g_T$ in an obvious notation. For example, when the field is along the c axis, $g_D=1.9574$ and $g_T=1.9894$, leading to $g_Z=2.021$. For a microwave frequency of 13.760 GHz, this corresponds to a field of 0.4865 T compared with the observed value of 0.4872 T [Fig. 4(a)]. When the field is perpendicular to the c axis $g_D=1.9556$ and $g_T=1.9825$ (average value), leading to $g_Z=2.0094$. This corresponds to a field of 0.4893 T at 13.760 GHz, which lies close to the partly resolved group of signals in the region between 0.4897 and 0.4902 T for $\theta=90°$ in Fig. 4(a). To within the accuracy to which the g values of center T can be determined, this agreement is satisfactory. It is also possible that the g values of the participating centers (especially the shallow donor) are altered slightly when they form an exchange coupled pair. The data are therefore consistent with center T consisting of an exchange-coupled pair of centers D and Z.

It is interesting to note that the zero-field parameters D and E are small relative to those observed for previously reported $S=1$ spectra in ZnO. For example, Galland and Hervé[39] found for holes located on two oxygen ions a distance 0.38 nm apart that D was 6.1 μeV, consistent with a magnetic dipole-dipole interaction between the two spins. The small values of D and E in the present case suggest either that the distance between the two coupled spins must be large (while at the same time being well defined) or that one of the spins is not strongly localized, which would be the case if, as suggested by the g values, it was associated with an electron bound to a shallow donor. The large linewidth of the Lorentzian components that we have used in order to simulate the spectra of center T could be accounted for by broadening due to a distribution of exchange energies between the exchange-coupled pairs at different separations[37] (leading to a distribution of values of the parameters D and E).

V. CONCLUSIONS

Optically detected magnetic resonance signals in epitaxial nitrogen-doped ZnO detected over the visible wavelength range show several signals, which can be distinguished on the basis of their laser power and angle dependences. However, none of these signals can be unambiguously identified as arising directly from the presence of nitrogen. The well-known shallow donor center was identified and three centers (Z, T, U) were observed, none of which however is directly attributable to point defects involving nitrogen. Of the centers, the g factors of one spin-1/2 center (Z) are unusual in

that $g_\perp < g_\parallel$, in contrast to those for hole centers previously reported, in which the holes are partly localized in oxygen *p* orbits. This leads to the proposal that the signal arises from a hole in a hybridized *s*-*d* state localized on a zinc atom in a interstitial site; the observed orthorhombic symmetry and *g*-tensor anisotropy are surmised to be the result either of a Jahn-Teller distortion or of the presence of a perturbing defect (such as a nitrogen at a nearby oxygen site). In view of the results of recent studies of electron-irradiated ZnO,[50] the latter model appears more probable. Since we do not observe the *Z* center in material that is not doped with nitrogen but which is otherwise prepared in the same way, we surmise that it either contains nitrogen (as discussed above) or that the presence of nitrogen favors its formation. The other spin-1/2 center (*U*) is only very weakly anisotropic and, at present, we do not have sufficient information to identify its microscopic nature. Finally, the spin–1 triplet center (*T*) is proposed to arise from a strongly exchange-coupled pair of donor (*D*) and *Z* centers; this interpretation is consistent with both the *g* factors and the symmetry of the observed ODMR spectra.

ACKNOWLEDGMENTS

We are grateful for the support from the EPSRC (Project No. GR/R34066), from the HEFCE (UK), and from Arima Optoelectronic (UK) Ltd.

*Electronic address: d.wolverson@bath.ac.uk; URL: http://staff.bath.ac.uk/pysdw

[1] H. Morkoç, in *Nitride Semiconductors and Devices*, Vol 32 of *Springer Series in Materials Science* (Springer, Berlin, 1999).
[2] Y. Chen, D. Bagnall, and T. Yao, Mater. Sci. Eng., B **B75**, 190 (2000).
[3] D. C. Look, Mater. Sci. Eng., B **B80**, 383 (2001).
[4] T. Dietl, Science **287**, 1019 (2000).
[5] W. Prellier, A. Fouchet and B. Mercey, J. Phys.: Condens. Matter **15**, R1583 (2003).
[6] K. Kosai, B. J. Fitzpatrick, H. G. Grimmeiss, R. N. Bhargava, and G. F. Neumark, Appl. Phys. Lett. **35**, 194 (1979).
[7] W. Stutius, Appl. Phys. Lett. **40**, 246 (1982).
[8] R. M. Park, H. A. Mar, and N. M. Salansky, J. Appl. Phys. **58**, 1047 (1985).
[9] R. M. Park, M. B. Troffer, C. M. Rouleau, J. M. Depuydt, and M. A. Haase, Appl. Phys. Lett. **57**, 2127 (1990).
[10] K. Ohkawa, T. Karawasa, and T. Mitsuyu, J. Cryst. Growth **111**, 797 (1991).
[11] K. Wolf, H. Stanzl, A. Naumov, H. P. Wagner, W. Kuhn, B. Hahn, and W. Gebhardt, J. Cryst. Growth **138**, 412 (1994).
[12] A. Kobayashi, O. F. Sankey, and J. D. Dow, Phys. Rev. B **28**, 946 (1983).
[13] Y. R. Ryu, S. Zhu, D. C. Look, J. M. Wrobel, H. M. Jeong, and H. W. White, J. Cryst. Growth **216**, 330 (2000).
[14] C. Morhain, M. Teisseire, S. Vézian, F. Vigué, F. Raymond, P. Lorenzini, J. Guion, G. Neu, and J.-P. Faurie, Phys. Status Solidi B **229**, 881 (2002).
[15] P. H. Kasai, Phys. Rev. **130**, 989 (1963).
[16] O. F. Schirmer, J. Phys. Chem. Solids **29**, 1407 (1968).
[17] R. T. Cox, D. Block, A. Hervé, R. Picard, C. Santier, and R. Helbig, Solid State Commun. **25**, 77 (1978).
[18] E.-C. Lee, Y.-S. Kim, Y.-G. Jin, and K. J. Chang, Physica B **308**, 912 (2001).
[19] H. Katayama-Yoshida and T. Yamamoto, Phys. Status Solidi B **202**, 763 (1997).
[20] M. Joseph, H. Tabata, and T. Kawai, Jpn. J. Appl. Phys., Part 2 **38**, L1205 (1999).
[21] S. B. Zhang, S.-H. Wei, and Y. Yan, Physica B **302**, 135 (2001).
[22] T. A. Kennedy and E. R. Glaser, in *Identification of Defects in Semiconductors*, Semiconductors and Semimetals Vol. 51A, edited by M. Stavola (Academic, San Diego, 1998), pp. 93–136.
[23] B. K. Meyer, Semicond. Semimetals **57**, 371 (1999).
[24] T. C. Damen, S. P. S. Porto, and B. Tell, Phys. Rev. **142**, 570 (1966).
[25] C. Solbrig, Z. Phys. **211**, 429 (1968).
[26] I. J. Broser, R. K. F. Germer, H. J. E. Schultz, and K. P. Wisznewski, Solid-State Electron. **21**, 1597 (1978).
[27] R. Kuhnert and R. Helbig, J. Lumin. **26**, 203 (1981).
[28] W. E. Carlos, E. R. Glaser, and D. C. Look, Physica B **308**, 976 (2001).
[29] F. Leiter, H. Zhou, F. Henecker, A. Hofstaetter, D. M. Hofmann, and B. K. Meyer, Physica B **308**, 908 (2001).
[30] N. Y. Garces, L. Wang, L. Bai, N. C. Giles, L. E. Halliburton, and G. Cantwell, Appl. Phys. Lett. **81**, 622 (2002).
[31] A. Abragam and B. Bleaney, *Electron Paramagnetic Resonance of Transition-Metal Ions* (Oxford University Press, Oxford, 1970).
[32] M. Schultz, Phys. Status Solidi A **27**, K5 (1975).
[33] C. Gonzalez, D. Block, R. T. Cox, and A. Hervé, J. Cryst. Growth **59**, 357 (1982).
[34] C. G. Van de Walle, Phys. Rev. Lett. **85**, 1012 (2000).
[35] S. F. J. Cox, E. A. Davis, S. P. Cottrell, P. J. C. King, J. S. Lord, J. M. Gil, H. V. Alberto, R. C. Vilao, J. Piroto Duarte, N. Ayres de Campos, A. Weidinger, R. L. Lichti, and S. J. C. Irvine, Phys. Rev. Lett. **86**, 2601 (2001).
[36] D. M. Hofmann, A. Hofstaetter, F. Leiter, H. Zhou, F. Henecker, B. K. Meyer, S. B. Orlinskii, J. Schmidt, and P. G. Baranov, Phys. Rev. Lett. **88**, 045504 (2002).
[37] D. Block, A. Hervé, and R. T. Cox, Phys. Rev. B **25**, 6049 (1982).
[38] J. E. Nicholls, J. J. Davies, B. C. Cavenett, J. R. James and D. J. Dunstan, J. Phys. C **12**, 361 (1979).
[39] D. Galland and A. Hervé, Phys. Lett. **33A**, 1 (1970).
[40] C. Gonzalez, D. Galland, and A. Hervé, Phys. Status Solidi B **72**, 309 (1975).
[41] J. M. Smith and W. E. Vehse, Phys. Lett. **31A**, 147 (1970).
[42] J.-M. Spaeth and H. Overhof, in *Point Defects in Semiconductors*, Vol. 51 of *Springer Series in Materials Science* (Springer, Berlin, 2003) p. 119.
[43] W. C. Holton, M. DeWitt, and T I. Estle, in *International Symposium on Luminescence*, edited by N. Richl and H. Kallmann

(Verlag Karl Thiemig, Munich, 1966), p. 454.
[44] D. J. Dunstan, J. E. Nicholls, B. C. Cavenett, and J. J. Davies, J. Phys. C **13**, 6409 (1980).
[45] J. Schneider, B. Dischler, and A. Räuber, J. Phys. Chem. Solids **31**, 337 (1970).
[46] N. Y. Garces, N. C. Giles, L. E. Halliburton, G. Cantwell, D. B. Eason, D. C. Reynolds, and D. C. Look, Appl. Phys. Lett. **80**, 1334 (2002).
[47] N. Y. Garces, L. Wang, N. C. Giles, L. E. Halliburton, G. Cantwell, and D. B. Eason, J. Appl. Phys. **94**, 519 (2003).
[48] J. S. Griffith, *The Theory of Transition Metal Ions* (Cambridge University Press, Cambridge, 1961).
[49] J. E. Wertz and J. R. Bolton, *Electron Spin Resonance* (McGraw-Hill, New York, 1972).
[50] Yu. V. Gorelkinskii and G. D. Watkins, Phys. Rev. B **69**, 115212 (2004).
[51] D. G. Thomas, J. Phys. Chem. Solids **3**, 229 (1957).
[52] K. Hoffmann and D. Hahn, Phys. Status Solidi A **24**, 637 (1974).
[53] M. Liu, A. H. Kitai, and P. Mascher, J. Lumin. **54**, 35 (1992).
[54] K. H. Chow and G. D. Watkins, Phys. Rev. Lett. **81**, 2084 (1998).
[55] K. H. Chow and G. D. Watkins, Phys. Rev. B **60**, 8628 (1999).
[56] G. D. Watkins and K. H. Chow, Physica B **273**, 7 (1999).
[57] D. C. Look, J. W Hemsky, and J. R. Sizelove, Phys. Rev. Lett. **82**, 2552 (1999).
[58] A. F. Kohan, G. Ceder, D. Morgan, and C. van de Walle, Phys. Rev. B **61**, 15 019 (2000).
[59] S. B. Zhang, S.-H. Wei, and A. Zunger, Phys. Rev. B **63**, 075205 (2001).
[60] F. Oba, S. R. Nishitani, S. Isotani, and H. Adachi, J. Appl. Phys. **90**, 824 (2001).
[61] N. O. Korsunka, L. V. Borkovska, B. M. Bulakh, L. Yu. Khomenkova, V. I. Kushnirenko, and I. V. Markevich, J. Lumin. **102**, 733 (2003).
[62] J. J. Davies and J. E. Nicholls, J. Phys. C **15**, 5321 (1982).
[63] J. J. Davies, R. T. Cox, and J. E. Nicholls, Phys. Rev. B **30**, 4516 (1984).